Orthopedic Screw Insertion Torque Prediction

Validation of a virtual mechanical test for the prediction of screw insertion torque in Sawbones® polyurethane foam in accordance to ASTM F543 standard

David Benoit, M.Sc. A, Franck Le Navéaux, Ph.D., Amy Posch, M.S., Julien Clin, Ph.D.

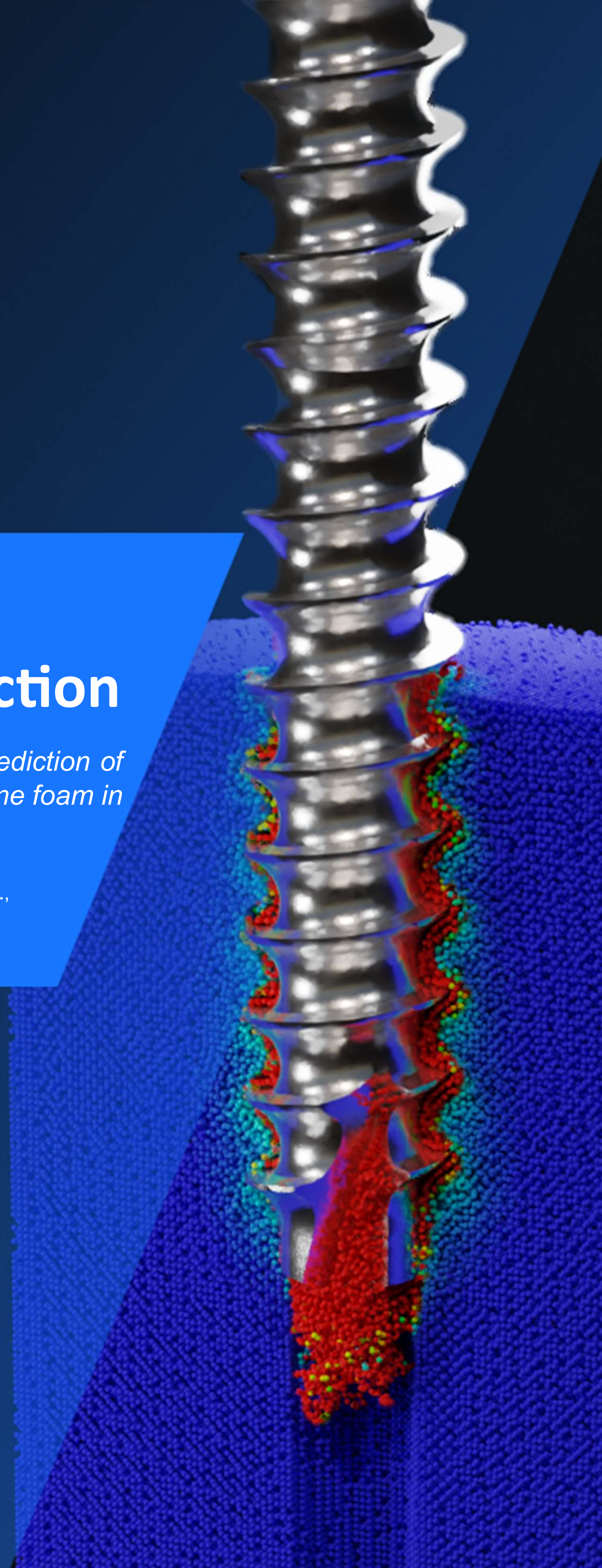

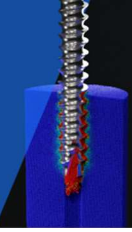

Introduction

Screws play a critical stabilizing role in orthopedic procedures, whether used alone or in combination with cage, plate, and rod systems. Most orthopedic screws are designed with a self-tapping feature to create threads within the bone while being inserted into a pilot hole that has been pre-drilled. When self-tapping screws are inserted into bone, they encounter resistance due to the cutting action of the screw threads and the generation of frictional forces caused by the compression of bone tissue against the threads and screw body. While adequate insertion torque can establish a strong connection by generating bone compression at the bone-screw interface (frictional locking), excessively high insertion torque can lead to bone failure, damage to the screw threads or head. This can weaken the integrity of the connection between the bone and the screw, ultimately compromising its ability to maintain a secure fixation or lead to complications should retrieval be necessary (Stoesz et al., 2014). High torque can also generate heat, causing thermal damage to the surrounding bone tissue and impairing the healing process (Paul et al., 2021). Therefore, it is crucial to carefully design screw features in order to achieve optimal insertion and fixation in various types of human bone tissues.

Although the orthopedic industry is putting significant effort into improving the performance of screws, several barriers hinder innovation. Due to the inherent variability in the specimen, experimental setup, measurements, and operational factors, traditional experimental testing may be limited when it comes to evaluating the impact of screw design feature modifications on performance. The assessment of insertion torque in cadaveric bone is notably impacted by the diverse mechanical properties exhibited by bone, influenced by factors such as age, gender, and health. Consequently, generalizing findings and comparing results across various studies becomes challenging. As a surrogate, synthetic bones made of rigid polyurethane foam allow for standardized testing conditions as they offer consistent mechanical properties. The polyurethane foam is designed to mimic the mechanical properties of trabecular and cortical bone (Calvert et al., 2010), and is recognized as a standard material for mechanical tests involving orthopedic devices, according to ASTM F1839 standard. Another limitation for innovation lies in the iterative process of designing, prototyping, testing and refining screw designs, which can be costly and time-consuming, hindering engineers' capability to reach optimal design.

Computational Modeling and Simulation (CM&S) provides an alternative to experimental testing and has the potential to be utilized to predict the insertion torque of self-tapping screws in the context of orthopedic implant research and development (R&D) and regulatory approval process. This approach offers the advantage of maintaining consistent testing conditions while providing valuable insights into the interaction of the screw and synthetic bone during insertion. A Finite Element Model (FEM) aiming to simulate the interaction between a screw and Sawbones® polyurethane foam during the insertion process as outlined in ASTM F543-A2 was consequently developed. In order to assess the FEM predictive capabilities, a comprehensive validation study was conducted to compare the simulated insertion torque with experimental measurements obtained under real-world conditions.

Objectives

To evaluate the predictive capability of a Screw Insertion Finite Element Model in determining the insertion torque required to insert screws into rigid polyurethane foam.

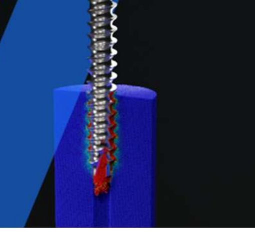

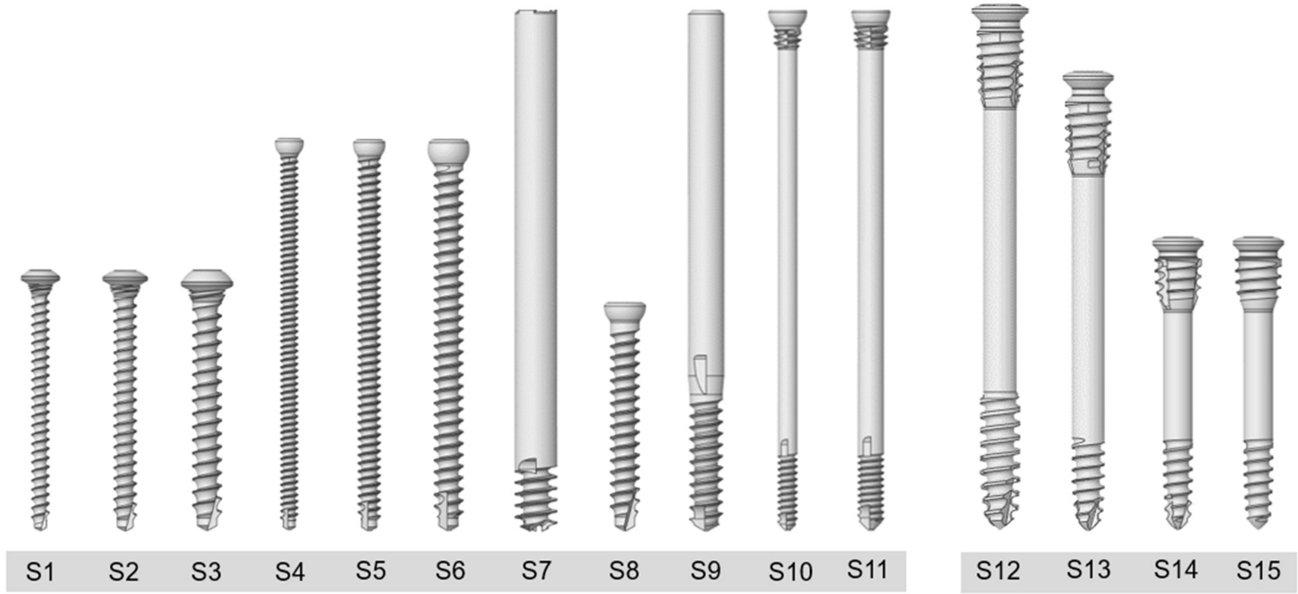

Figure 1: Sample of orthopedic screws included in the validation study divided into two distinct groups based on their surface finishes.

Material and methods

The predictions of the Screw Insertion FEM were compared to experimental tests across a wide variety of orthopedic screw designs and insertion scenarios. In this blinded comparative study, experimental and numerical tests were conducted by two separate operators.

Orthopedic screw samples

Fifteen self-tapping orthopedic screws (S1 to S15) and their associated 3D models were obtained from two implant manufacturers (Figure 1). The screws were separated into two distinct groups based on their surface finishes. S1 to S11 screws underwent electropolishing surface treatment in accordance with ASTM B912 standard, while S12 to S15 screws did not undergo any surface treatment process after fabrication but had a requirement for roughness average (R_a) < 63 µm. The screws were selected to encompass a wide range of geometric features and designs among orthopedic screws (Figure 2), allowing an extensive assessment of the predictive capabilities of the FEM. Screws core diameter varied from 1.8 to 4.7 mm and outer thread diameter varied from 2.7 to 6.5 mm. Pitch

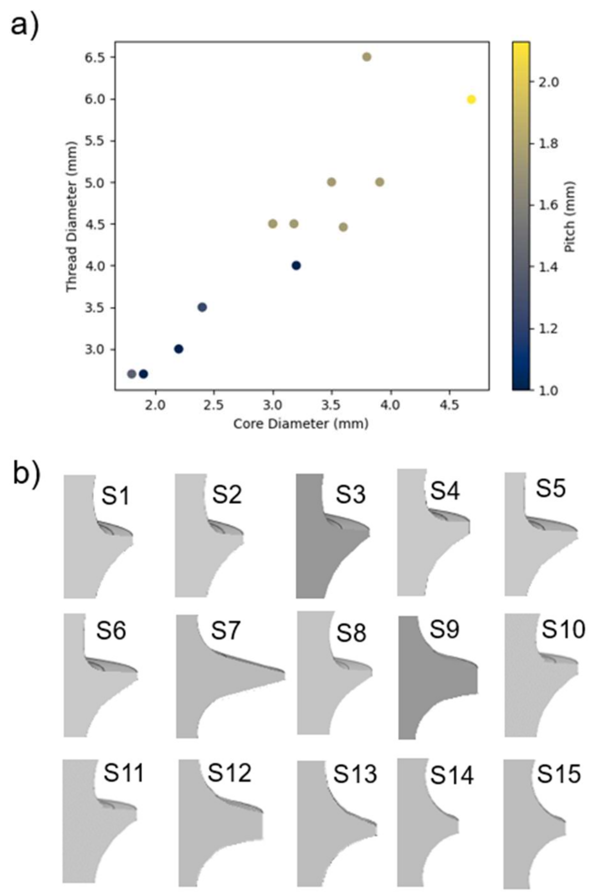

Figure 2: a) Screw geometric features design space. b) Screw thread profiles (scaled).

varied from 1 to 2.13 mm. The thread profiles of the screws varied between standard buttress threads and different variations of rounded V-thread. S1 to S11 screws had a cylindrical core diameter while S12 to S15 screws had a tapered core diameter. Both S14 and S15 screws had similar characteristics, except for the presence of a cutting flute feature in S14, which was absent in S15.

Experimental testing

Experimental evaluation of the insertion torque for each screw was conducted following ASTM F543-A2 methods. Solid polyurethane foam blocks of grade 20 PCF density were obtained from Sawbones® (Sawbones, Pacific Research Laboratories, WA, USA) and the apparent density of each block was determined according to ASTM D1622.

The pilot holes in the foam blocks were drilled using standard-sized drill bits, specifically chosen to be the closest to, but slightly smaller than, the core diameter of the screws. This selection ensures a proper fit during the insertion process. Screw insertion was performed perpendicularly to the blocks using a motorized torque test stand (Mark-10 TSTM-DC-1) at a rotation rate of 3 RPM (Figure 3).

Figure 3: Screw insertion with Mark-10 TSTM-DC-1.

A manual vertical force was initially applied on the screws to ensure it was properly engaged in the foam block and a 7N axial load was maintained throughout the remainder of the insertion process. Final insertion depth was measured after each test and the torque-rotations relationships obtained from the torque sensor were converted to torque-insertion depth relationships. Insertion tests were repeated five times per screw to account for experimental variability.

Screw Insertion FEM

The Screw Insertion FEM was developed using LS-DYNA explicit solver (Ansys, Canonsburg, Pennsylvania, USA). The polyurethane foam material properties were obtained from compressive (ASTM D1621), tensile (ASTM D1623), shear (ASTM C273) and custom indentation tests (Figure 4).

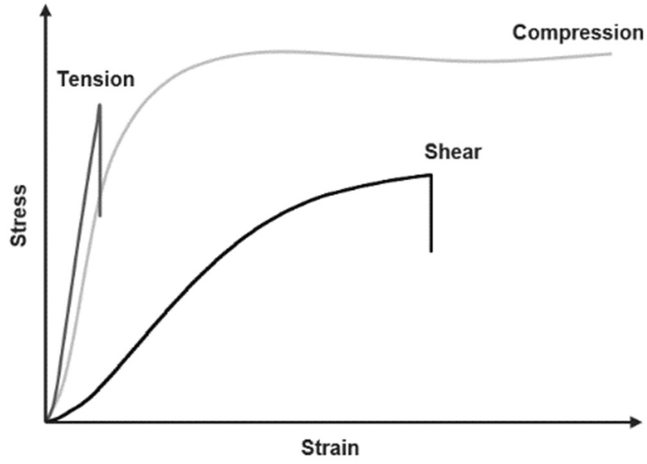

Figure 4: Grade 20 PCF stress strain relationship.

An elasto-plastic constitutive law was utilized to model the nonlinear behavior of the polyurethane foam material, and FEMs replicating each test were created to calibrate the virtual foam material properties.

Due to the limitations of conventional mesh-based approaches in capturing the complex behavior of material failure in cases involving penetration and crushing, a meshless particle method was utilized to model the polyurethane foam. The particle method offers several advantages over traditional mesh-based approaches as it allows to accurately simulate moving discontinuities and debris from failure with mass conservation, and has the ability to handle extremely high deformations without stability issues. The screws were modeled using a mesh-based approach to ensure an accurate representation of their geometrical features.

For each screw, a FEM replicating the ASTM F543-A2 insertion experimental set-up was created. The screws were initially positioned above the polyurethane foam blocks. The sides of the blocks were constrained to prevent any movement, while the screws were restricted to only allow translation and rotation along their main axis. The screws were defined as rigid bodies due to their stiffness being orders of magnitude higher than those of the polyurethane foam. The screw-foam interface was modeled using a node-to-surface penalty method. Rotational and translational velocities were applied on the screw, simulating the insertion torque applied by the motorized torque test stand.

To ensure an accurate comparison between the predicted torque-insertion depth relationships generated by the model and the corresponding experimental data, a phase correction was implemented to account for the initial penetration of the screws into the pilot holes before activating the motorized torque test stand. This correction involved superimposing the final simulated depth of insertion onto the final experimental depth of insertion, allowing to compare the insertion torque for the same position of the screws within the foam blocks.

An uncertainty quantification study was conducted on the friction coefficient value between the screw and foam. The influence of this parameter on the insertion torque was found to be significant. Accurately determining the coefficient of friction between the screws and polyurethane foam through experimental means presents significant challenges as standard experimental tests used to determine this parameter are typically not well-suited for the complex geometry of screws. Therefore, the coefficient of friction was calibrated on a single screw from both groups (S1 and S12) to match experimental test data. This parameter then remained constant for all other tested screws of the same group (S2 to S11 and S13 to S15 respectively) which had the same surface finish.

A sensitivity analysis was conducted on key FEM numerical parameters. Particle size was refined through a convergence study to ensure numerical accuracy and was adapted based on screw features size. Contact penalty stiffness was defined as the minimum value at which there was negligeable element penetration and no effect on the torque-insertion depth curves. To minimize computational time, a sensitivity analysis was performed to determine the highest rotational velocity at which there was negligeable alterations of the results.

Model Prediction Evaluation

The correspondence of the FEM with the experiments was evaluated using two different methods: the Correlation and Analysis (CORA) metric and the torque-insertion depth relationship slope.

The CORA analysis was performed to assess the agreement between the simulated and experimental torque-insertion depth relationships (Gehre et al., 2009). Three CORA criteria were utilized: corridor rating, shape rating, and size rating. The corridor rating was assigned a value of 1 if the simulation results fell within one standard deviation of the average curve obtained from 5 test repetitions, 0 if outside two standard deviations, and a linearly interpolated value between 0 and 1 for results between one and two standard deviations. The overall corridor rating was obtained by averaging the ratings for each data point. The size rating and shape rating were determined following (Barker et al., 2017). The size rating (Eq. (1)) compares the area under the simulation curve $y(t)$ and the experimental curve $x(t)$, with the larger value serving as the denominator. The shape rating (Eq. (2))

compares the slope and its changes between the simulated curve y(t) and the experimental curve x(t). The phase-shifting was not considered in this rating calculation as both experimental and simulated response were already superimposed from insertion depth measurements. The result of the CORA analysis is a numerical value between 0 and 1 determined by averaging the three criteria and represents the level of agreement between the datasets. The suggested interpretation of the ratings is: excellent (0.86–1), good (0.65–0.86), fair (0.44–0.65), marginal (0.26–0.44), and unacceptable (0–0.26) (Cesari et al., 2001).

$$(1)\ CORA_{size} = \frac{\sum_{i=1}^{n} y^2(t_{min}+i*\Delta t)}{\sum_{i=1}^{n} x^2(t_{min}+(m+i)*\Delta t)}$$

$$(2)\ CORA_{shape} = \frac{\sum_{i=0}^{n-1} x(t_{min}+(m+i)*\Delta t)*y(t_{min}+i*\Delta t)}{\sum_{i=0}^{n-1} x^2(t_{min}+(m+i)*\Delta t)*\sum_{i=0}^{n-1} y^2(t_{min}+i*\Delta t)}$$

For the torque-insertion depth relationship slope, the starting point for slope calculation was defined as the depth of insertion at which the screws achieved proper stable engagement within the foam blocks, exhibiting a steady quasi-linear or exponential increase in slope. The termination point for slope calculation was determined as the endpoint of the torque as a function of screw insertion depth curve (Figure 5).

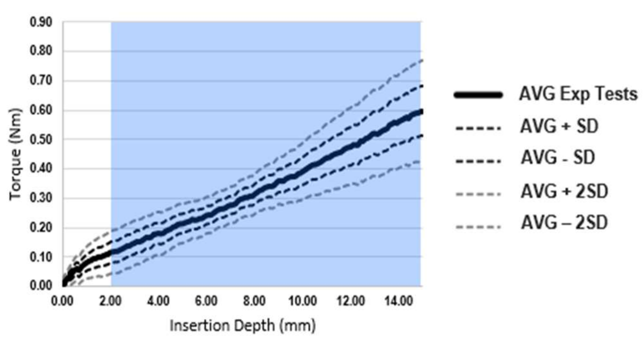

Figure 5: Section of the curves used for slope calculation.

For tapered screws exhibiting a non-linear torque-insertion depth relationship, the mean slope between the starting and termination points was considered.

Pilot hole sensitivity evaluation

To further evaluate the model's predictive capability, the impact of pilot hole size on the insertion torque for a specific screw sample (S9) was investigated. The study involved assessing and comparing the experimental results and model predictions for three different pilot hole sizes, namely 3/32", 7/64", and 1/8".

Results

Sawbones® material characterization

The polyurethane foam blocks utilized for the experimental tests had a density of 315.6 kg/m3 (19.7 PCF), falling within the range of 20 PCF specified by the ASTM F1839 (288.5 to 352.5 kg/m3).

Coefficient of friction calibration

Through a calibration study conducted on screw samples S1 and S12, the impact of varying the coefficient of friction between 0.05 and 0.40 was assessed (Figure 6). This parameter was defined as 0.09 for screws that underwent electropolishing surface treatment (S1 to S11) and 0.15 for screws did not undergo surface finish treatment (S12 to S15). Those friction coefficients yielded the best fit between the experimental measurements and the simulated results.

Model Predictive capability

Following the initial few millimeters of insertion, where proper engagement of the screw threads in the foam blocks was achieved, torque-insertion depth relationships demonstrated a quasi-linear increase in torque for cylindrical screws and an exponential increase for screws with a tapered core, behavior that was captured by the model (Figure 7). The experimental measurements and

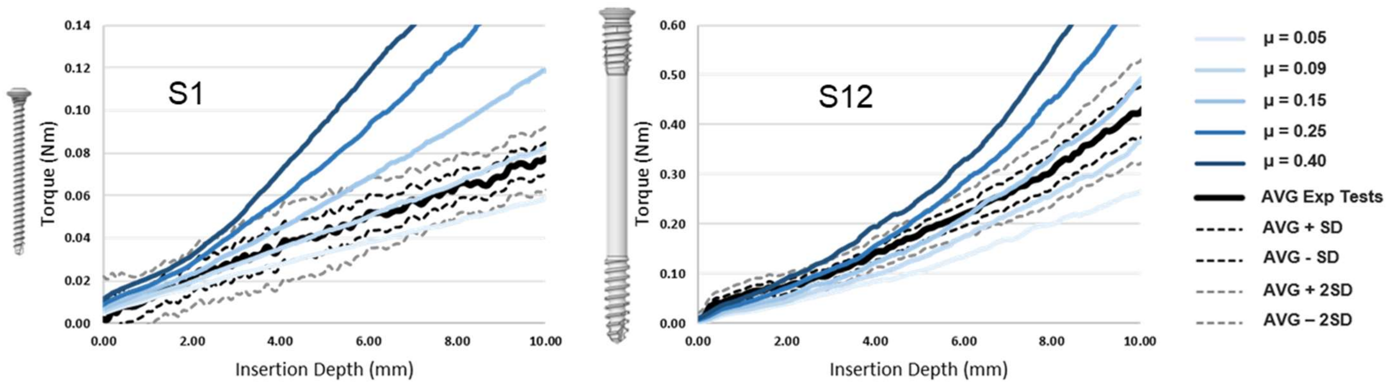

Figure 6: Coefficient of friction calibration for both groups of screws with different surface finish.

simulated predictions displayed similar patterns across all tested screws, with a slight deviation observed for S7 where the model predicted a steeper slope in its torque-insertion depth curve compared to the experimental measurements. The corridor, shape, size, and resulting CORA scores are reported in Figure 8. CORA scores for all tested configurations varied between 0.68 and 0.97 with an average value of 0.86. The measured and predicted torque-insertion depth slopes are presented in Figure 9. Across all tested screws, the mean slope ranged from 0.0078 to 0.0628 Nm/mm, with an average variability of ±17.7% for the 5 repetitions. The

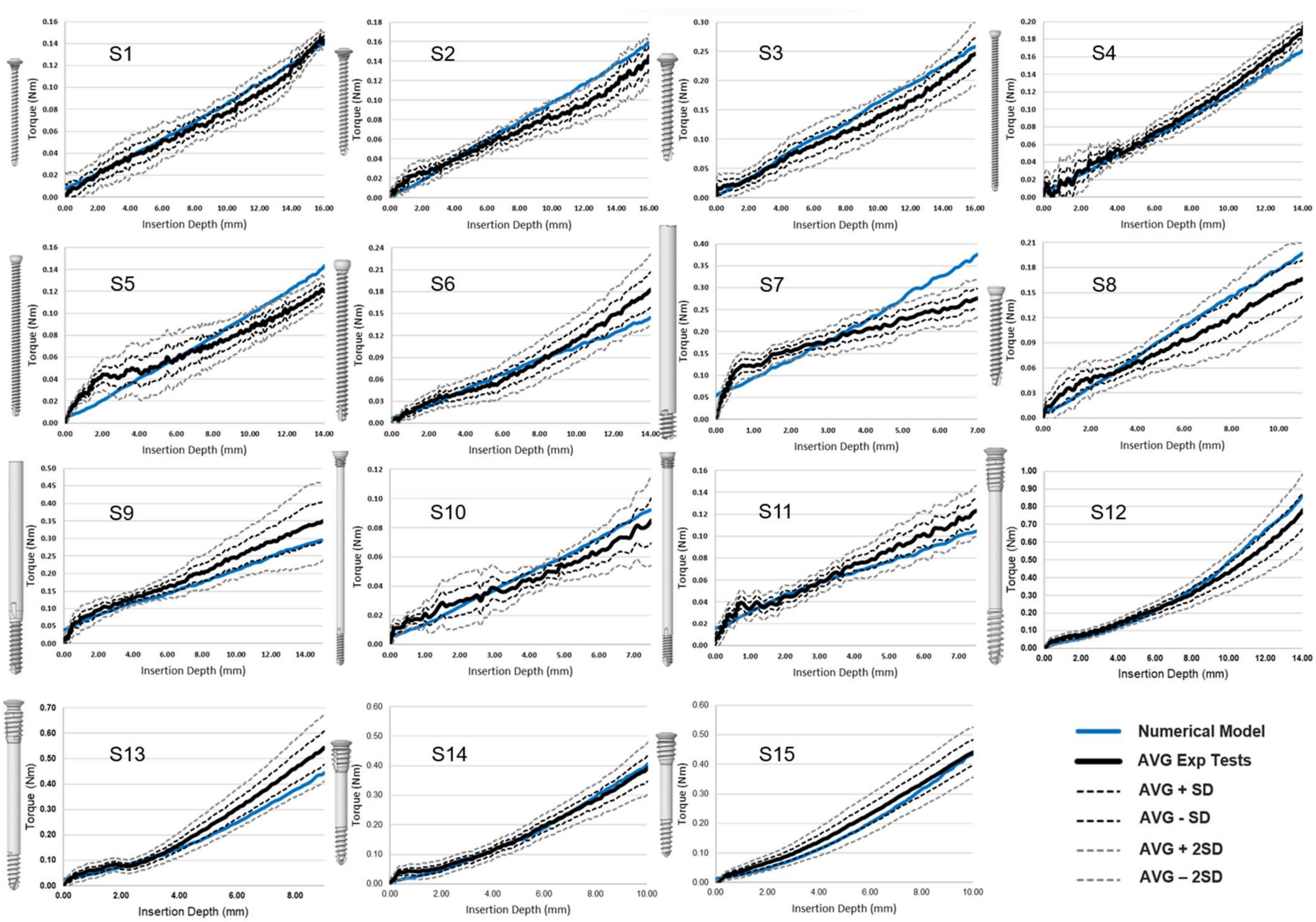

Figure 7: Experimental results and simulated predictions for all tested screws.

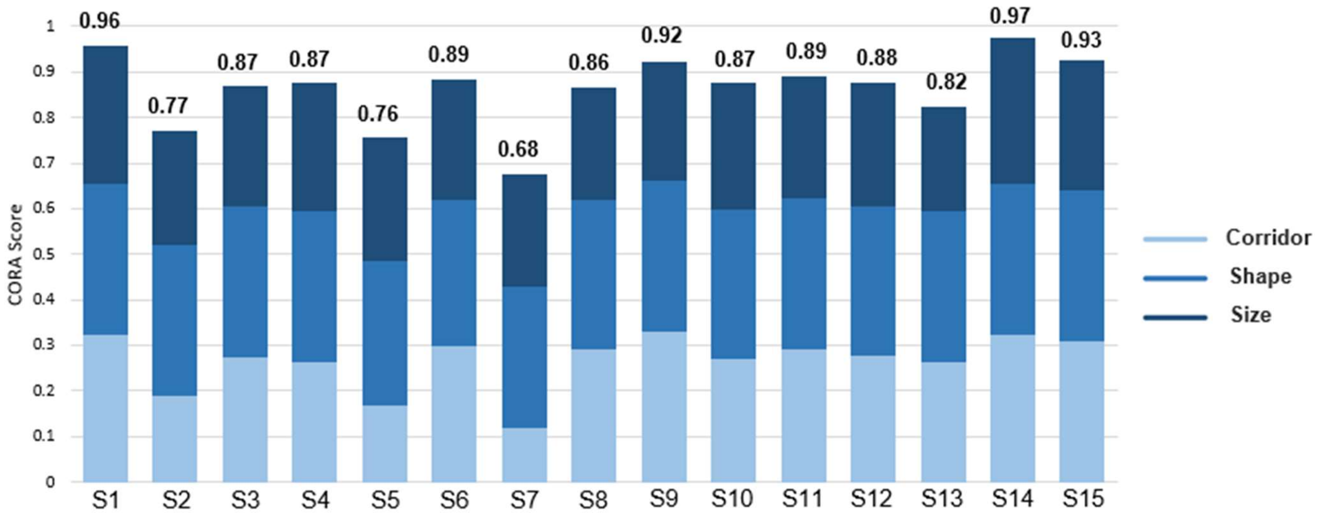

Figure 8: Corridor, shape, size and resulting CORA score for all tested screws.

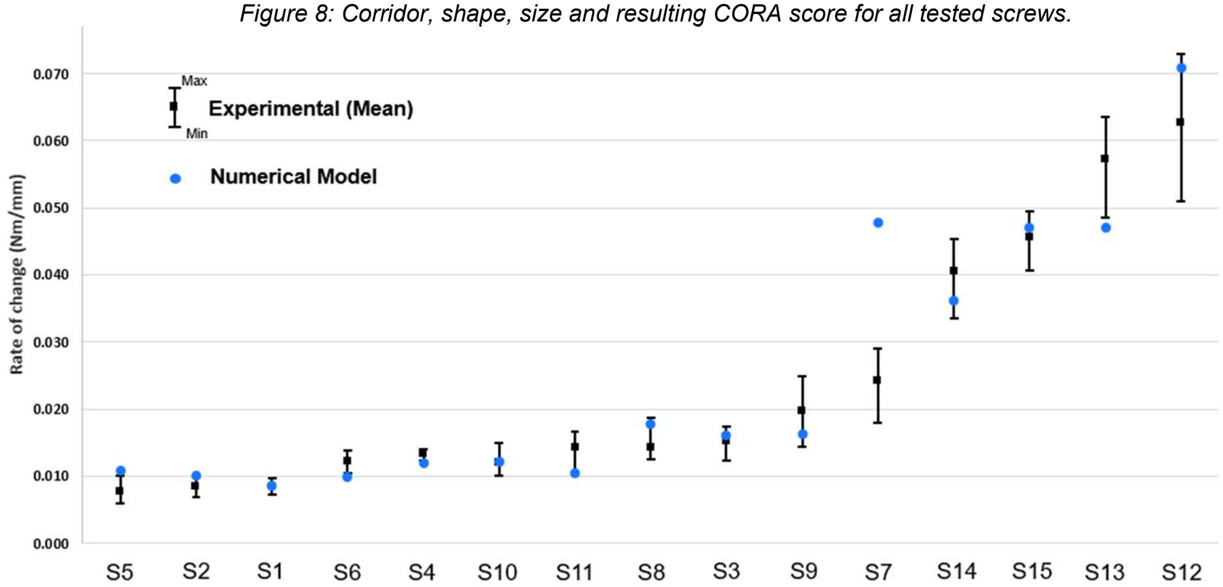

Figure 9: Measured and predicted torque-insertion depth slopes for all tested screws.

mean absolute error prediction for the Screw Insertion FEM was 20.2%, with ten out of fifteen predictions falling inside the experimental variability range. S4, S5, S6, S7 and S13 screws deviated beyond the experimental range by 3.3%, 7.1%, 6%, 39% and 3.3%, respectively.

Pilot hole sensitivity evaluation

The torque required to insert a screw into foam blocks was found to be influenced by the diameter of the pilot hole, which was accurately predicted by the numerical model (Figure 10). CORA scores were 0.92, 0.88 and 0.86 for pilot hole diameters of 3/32”, 7/64” and 1/8”, respectively. The measured and predicted torque-insertion depth slopes for the three pilot hole diameters are presented in Figure 11. From a pilot hole of 1/8’’ to 7/64’’ and from 7/64’’ to 3/32’’, the mean slope increased by 84% and 3.5% respectively. All FEM predictions were inside the experimental variability range.

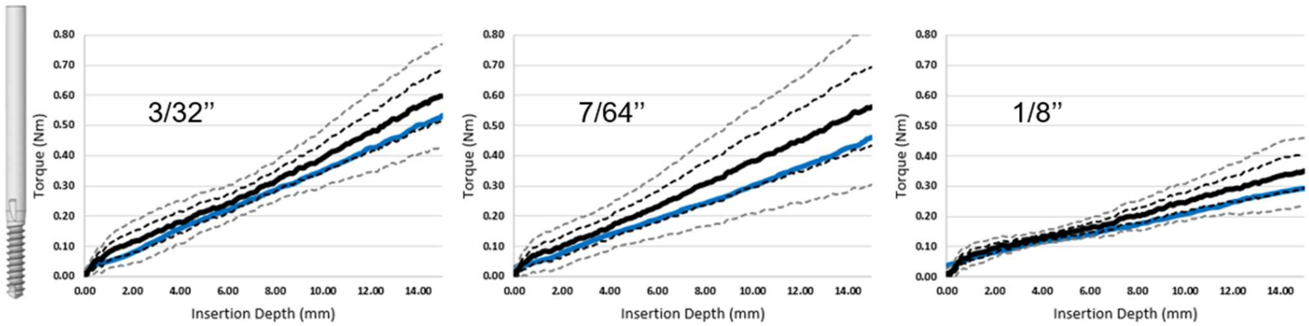

Figure 10: Experimental results and simulated predictions for S9 screw inserted into 3 pilot holes of various diameters.

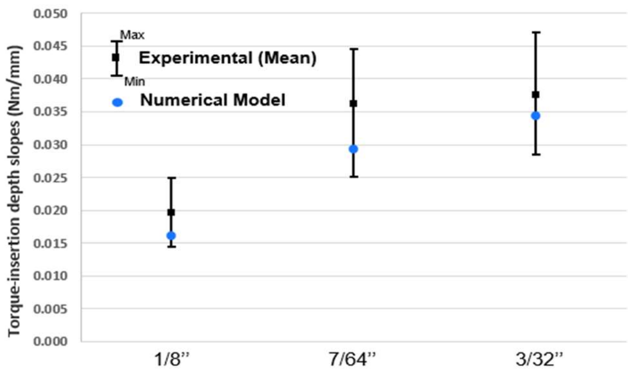

Figure 11: Measured and predicted torque-insertion depth slopes for S9 screw inserted into 3 pilot holes of various diameters.

Discussion

The objective of this study was to assess the ability of a computational model to predict the insertion torque during the insertion of orthopedic screws in synthetic bone. To assess the model's performance, a diverse range of screws with varying sizes and thread shapes were selected. The impact of a cutting flute feature was evaluated through the selection of S14 and S15 screws, which shared identical characteristics except for the presence of a cutting flute in S14 and its absence in S15, which allowed to isolate and assess the model's predictive accuracy specifically for this feature. Finally, the model's ability to predict the insertion torque for different pilot hole sizes was evaluated. By encompassing such a wide design space, this study aimed to provide robust evidence of the model's capability to predict the insertion torque as per the ASTM F543-A2 standard.

The accuracy of the Screw Insertion FEM in predicting the insertion torque was evaluated through two different analyses, the CORA metric and the torque-insertion depth relationship slope. By incorporating both analyses, this study accounts for the limitations of each method in comparing the full torque-insertion depth relationships and provides a comprehensive assessment of the model's accuracy. The CORA scores ranged from 0.68 to 0.97 with a mean of 0.87 for all tested configurations, demonstrating a high level of agreement between the experimental and predicted data. When considering the slope of the torque-insertion depth relationship, the model's prediction accuracy aligned closely with the experimental test results, highlighted by the majority of tested configurations falling within the range of experimental variability. Furthermore, the numerical model accurately predicted the influence of pilot hole diameters on the torque required for screw insertion into foam blocks, demonstrating its ability to capture the complex interaction between the screw, pilot hole, and surrounding material. However, the S7 screw simulation exhibited lower accuracy compared to the other predictions. This screw was characterized by the largest thread diameter and by a particular cutting feature with three dents. No correlation was found between the thread size and the predictive error observed in other tested configurations. Further investigation is required in this case to identify factors contributing to the lower prediction accuracy. Despite this outlier, the overall performance of the Screw Insertion Model, as evidenced by the CORA scores and the rate of torque change analysis, highlights its robustness and reliability in predicting the torque-insertion depth relationships across a wide range of screw configurations.

The study revealed the crucial influence of the coefficient of friction between the foam material and screws on the insertion torque. Accurately characterizing this coefficient through experimental means can be challenging, primarily due to the limitations of standard experimental tests when applied to complex geometries. The model's predictive utilization can be challenging when there is no prior knowledge of the precise value of the coefficient of friction. In the present study, the coefficient of friction for electropolished surface was determined to be 0.09, which closely aligns with the value of 0.08 reported for polished titanium (Grant et al., 2007). For the set of screws which did not undergo surface treatment, a friction coefficient of 0.15 was determined. To harness the predictive capabilities of the model for screws with unknown coefficients of friction with foam material, a similar calibration approach can be employed by utilizing available experimental data obtained from a screw manufactured with a comparable surface treatment. By leveraging this existing knowledge and establishing a correlation between surface treatment and coefficient of friction, the model can be adjusted to better estimate the insertion torque during screw insertion. Otherwise, conducting comparative analysis still provides valuable insights for evaluating different screw designs. Even in the absence of an exact insertion-torque relationship prediction, determining the relative performance or identifying the worst-case configuration among multiple screw designs remains valuable and can substantially expedite the development process. Further work is necessary to provide comprehensive guidelines for future users of the Screw Insertion Model to determine relevant friction coefficient values of their specific implant and manufacturing processes.

The process of experimentally testing screw insertion torque has certain limitations, including inherent variability in the results observed across different tests, both intra and inter laboratories. In the current study, the experimental slope measurements revealed a notable degree of variability among the samples, which can be attributed to several factors. One significant factor is the initial instability observed during the insertion process, particularly when the screw threads are not yet properly engaged in the foam block, which may lead to slight variations of screw alignments between repetitions. Additionally, pilot hole preparation has been shown to play an important role in the insertion torque of a screw. Although increasing the number of repetitions can improve the statistical reliability of results, it also extends the duration of testing, which can be time-consuming and costly. The Screw Insertion FEM offers a consistent and standardized method for evaluating screw insertion torque by providing a fully controlled testing environment that minimizes sources of variability found in experimental testing. Combining the advantages of the particle method to simulate the extremely large deformations and compaction of the foam and the exact geometry of the screws through a conventional mesh-based approach allowed to enhance the overall accuracy and fidelity of the analysis. The standardized testing conditions provided by the Screw Insertion FEM are ideal for conducting design of experiment types of studies, enabling a clear understanding of the impact of each screw design parameters on performance. Additionally, the use of this numerical model can significantly reduce the time and resources required for prototyping and testing new designs, making it an efficient tool for the optimization of orthopedic screws.

Conclusion

This study demonstrates that the Screw Insertion Finite Element Model is a high-potential tool for evaluating the insertion torque of orthopedic screws in synthetic bone material. By conducting an in-depth analysis of the torque-insertion depth relationships, the model demonstrated a high level of agreement between the experimental and predicted data across a wide range of test configurations. The standardized testing environment provided by the Screw Insertion Model can significantly reduce the time and resources required for evaluating new screw designs and could be used as a complementary or surrogate tool to the ASTM F543 bench-top tests. The model and testing set-up could be adapted to other ASTM tests conducted on synthetic bone material, expanding its potential applications in the orthopedic field.

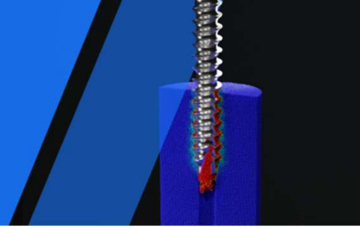

References

ASTM B912-02. Standard Specification for Passivation of Stainless Steels Using Electropolishing (ASTM International, West Consho- hocken, PA, 2018).

ASTM C273-20. Standard Test Method for Shear Properties of Sandwich Core Materials (ASTM International, West Consho- hocken, PA, 2020).

ASTM D1621-16. Standard Test Method for Compressive Properties of Rigid Cellular Plastics (ASTM International, West Consho- hocken, PA, 2016).

ASTM D1622-14. Standard Test Method for Apparent Density of Rigid Cellular Plastics (ASTM International, West Conshohocken, PA, 2014).

ASTM D1623-17. Standard Test Method for Tensile and Tensile Adhesion Properties of Rigid Cellular Plastics (ASTM International, West Consho- hocken, PA, 2017).

ASTM F1839-08. Standard Specification for Rigid Polyurethane Foam for Use as a Standard Material for Testing Orthopaedic Devices and Instruments (ASTM International, West Conshohocken, PA, 2008).

ASTM F543-17. Standard Specification and Test Methods for Metallic Medical Bone Screws (ASTM International, West Consho- hocken, PA, 2017).

Barker, J. B., Cronin, D. S., & Nightingale, R. W. (2017). Lower cervical spine motion segment computational model validation: Kinematic and kinetic response for quasistatic and dynamic loading. Journal of Biomechanical Engineering, 139(6), 1–11. https://doi.org/10.1115/1.4036464

Calvert, K. L., Trumble, K. P., Webster, T. J., & Kirkpatrick, L. A. (2010). Characterization of commercial rigid polyurethane foams used as bone analogs for implant testing. Journal of Materials Science: Materials in Medicine, 21(5), 1453–1461. https://doi.org/10.1007/s10856-010-4024-6

Cesari, D., Compigne, S., Scherer, R., Xu, L., Takahashi, N., Page, M., Asakawa, K., Kostyniuk, G., Hautmann, E., Bortenschlager, K., Sakurai, M., & Harigae, T. (2001). WorldSID Prototype Dummy Biomechanical Responses. SAE Technical Papers, November. https://doi.org/10.4271/2001-22-0013

Gehre, C., Gades, H., & Wernicke, P. (2009). Objective rating of signals using test and simulation responses. 21st International Technical Conference on the Enhanced Safety of Vehicles Conference (ESV), 9–407.

Grant, J. A., Bishop, N. E., Götzen, N., Sprecher, C., Honl, M., & Morlock, M. M. (2007). Artificial composite bone as a model of human trabecular bone: The implant-bone interface. Journal of Biomechanics, 40(5), 1158–1164. https://doi.org/10.1016/j.jbiomech.2006.04.007

Paul, B., Frank, A., Raschke, M. J., & Wähnert, D. (2021). Local heat generation during screw insertion into diaphyseal bone: a biomechanical study on different conditions (e.g. screw type, material, mode of insertion). BMC Musculoskeletal Disorders, 22(1), 1–10. https://doi.org/10.1186/s12891-021-04723-6

Stoesz, M. J., Gustafson, P. A., Patel, B. V., Jastifer, J. R., & Chess, J. L. (2014). Surgeon perception of cancellous screw fixation. Journal of Orthopaedic Trauma, 28(1), 1–7. https://doi.org/10.1097/BOT.0b013e31829ef63b

About the authors

David Benoit, M.Sc. A, is Biomechanical Simulation Specialist at Numalogics

Corresponding author: dbenoit@numalogics.com

Franck Le Navéaux, Ph.D., is Scientific Research Manager at Numalogics

Amy Posch, M.S., is Biomechanical Engineer at Sawbones

Julien Clin, Ph.D., is Director of Biomechanical Simulations R&D at Numalogics

SAWBONES®

About Sawbones®

In addition to supplying the world's best medical procedure simulation models, Sawbones® offers a complete range of bones and test materials for orthopaedic experimental and computer simulated biomechanics. Designed to simulate the physical properties of human bone; these materials offer a more reliable test bed for biomechanical studies than cadaveric specimens. As a contributor to the orthopaedic research community, Sawbones® has been qualifying and using biomechanical test materials for over 30 years with their use becoming more prevalent in scientific journals. Sawbones® are an active member of ASTM and ISO subcommittees for medical devices and implants for surgery.

www.sawbones.com

numalogics

About Numalogics Inc.

Numalogics, specializes in computer modeling and simulation for the medical device, sports equipment, and military industries. In addition to providing consulting services that can help solve product development and innovation challenges, Numalogics is carving a path to develop easy-to-use software applications that would allow product innovators to perform simulation testing, without requiring the dedicated skill and experience in computer simulation. To ensure models are verified and validated, Numalogics is an active member of the ASME V&V 40 committee.

www.numalogics.com